Synthesis of Nano particle ZnO-organic Nanohybrid and its role in Controlled Release of 4-Chlorophenoxy Acetate from the lamella of ZnO nanocomposite

تحضير جزيئات نانوية بين اوكسيدالزنك وجزيئات عضوية من خلال التهجين ودورها في عمليه السيطرة علئ تحرر 4-كلور فينوكسي حامض الخليك.

Abbas Matrod Bashi

Chemistry Department, College of Pharmacy, Karbala University, Karbala, Iraq

Abstract

Direct intercalation of 4-Chlorophenoxyacetate into ZLH interlayer was obtained by reacting ZnO with 4-Chlorophenoxyacetic acid. The resulting Nanohybrid material is white needle like-crystals with two phases at 21.25 and 18.69 Å respectively. This was characterized using XRD. SEM and TEM to show a fibrous nonohybrid structure. The controlled release study showed that within 2000 min. the accumulation of 4-Chlorophenoxyacetate is 94% and t ½ value of 990 min. That is an indication, ZnO can be used to study the controlled release delivery of herbicide active molecules.

Keywords: Herbicides, 4-chlorophenoxy acetic acid, ZnO, control release, intercalation

الخلاصة:

من خلال طريقة التبادل الايوني المباشر بين 4-كلور فينوكسي حامض الخليك واوكسيد الزنك, حصلنا علئ نواتج ذات بلورات بيضاء ابرية نانومترية, هذه البلورات تكونت بسرعتي تبادل مختلفتين مما ادئ الئ تكوين طورين 21.25 و 18.69 انكستروم علئ التوالي من خلال تشخيصها بواسطة تقنية الاشعة السينية والمايكروسكوب الالكتروني.

تم دراسة حركية تحرر الايون 4-كلور فينوكسي حامض الخليك من بين الطبقات بتاثير الوسط المائي لكاربونات الصوديوم فوجد انه يخضع الئ معادلة الرتبة الثانية وان نسبته الماوية هي 94% . هذه النتائج تشير الئ امكانية استخدام اوكسيد الزنك في التحضير والسيطرة علئ تحرير المركبات النانومترية والتي تستخدم كمبيدات ادغال وهذا يقلل من عملية التلوث البيئي للتربة والمياه.

1.0 Introduction

Zinc oxide nanoparticles exhibit a wide range of applications due to their electrical and optical properties which are dependent on both shape and size. The development of synthetic method to control these parameters is the key to understanding the mechanism of nanoparticle formation. New particle ZnO is one of multifunctional nanomaterials which has promising applications such as Zinc-layered-galate salts [1], the effect of polymer on to the size of zinc layered hydroxide[2], the antibacterium [3], In the synergistic cytotoxic effect on dannorubicin [4]. ZnO was synthesised by hydrozincite [5] a direct LDH-d-guconate intercalations was produce a nano particle [6]. ZnO nanofiber was synthesised by Carbonization [7]. Also it was prepared as a nanoarrays by polyacrylonitrile via sonochemical rout [8]. Magnetic nanoparticles have been synthesized by a co-precipitation method to form Fe_3O_4/ZnO [9], biomineralized ZnO particles in spider silk peptide were done [10]. Conjugated polymer with ZnO has been prepared as nanocomposites [11], surfactant –ZnO nanocrystals for photo catalyst degradation of organic-dyes was prepared [12]. Controlled release technologies have emerged as an approach to solve the problem of contamination with herbicides used as plant growth regulator by intercalation [13, 14]. The work reported here is on the intercalation of 4CPA into Zinc layered hydroxide by reaction of 4-Chlorophenoxyacetic acid with ZnO for the formation of novel zinc-4CPA-layered hydroxide nanohybrid)(ZCN). The resulting material was subsequent used as controlled release formulation of interlamellae .

2.0 **Materials and Methods**

ZnO from Acrose and 4-chlorophenoxy acetic acid (4CPA) from Merck were used without further purification. 4CPA, having the following molarities (0.05, 0.1, 0.2, 0.4M) was dissolved in 50 ml of 90 % ethanol. Each solutions was added to 0.5gm ZnO in a conical flask and 1ml HCl (0.05M) was then added to serve as competitor ion with the organic ions under N_2 gas, stirred for two hours and aged at 70 C^o for 18 hours. The precipitate was then cooled, centrifuged and washed four times with deionized water, dried in an oven at 70C^o, and stored in a sample bottle for further use and characterizations .

3.0 **Results and Discussion**

3. 1 **Characterizations**

X-Ray powder diffraction patterns (PXRD) were obtained with a Shimadzu XRD-6000 powder diffractometer using (λ=1.540562 Å) at 40 kW and 30 mA, scan rate = 0.5 degrees/min.

Fourier transform infrared (FTIR) spectra were recorded by using a spectrophotometer thermo Nicolet Ft-IR Nexus at wave number range between 4000-400 cm^{-1} range. The CHNS analyzer, model CHNS-932 (LECO) was used to determine the percentage of 4CPA. The TG/DTG was carried out with a Setaram TG-DSC-11 apparatus with fully programmable heating and cooling sequence sweep gas valve switching and data analysis. The surface morphology and bulk structure of the sample were observed using a scanning electron microscope (SEM) model JOEL (JSM-6400) and TEM (Hitachi H7100).

3.2 **XRD Powder X-Ray diffraction**

Powder X-Ray diffraction patterns of (ZCN), obtained from reaction between ZnO and 4CPA are shown in Fig. [1]. All the samples show sharp diffracted peaks indicated well ordered and highly crystalline materials. The intercalation of 4CPA anion resulted in an expansion of the basal spacing of Zinc-layered-hydroxide. This is due to the size and spatial orientation of the 4CPA anion inside the inorganic zinc layered hydroxide interlamelar of ZLH.

A closer look the PXRD diffraction pattern shows that intercalation of 4CPA shows well ordered biphasic nanohybrid with two phases at 21.25 to 18.69 Å respectively we labeled here as phase (a) and (b). The observation of the other harmonics (003), (006) and (009) for phase (a) with interlayer spacing d value is 21.25, 10.54, 5.72 Å, respectively. For phase (b) the (003, 006, 009), d value is 18.69, 9.44, 4.7 Å respectively. These two phases may have resulted from two different phases growth in the same time depending on the initial concentrations of the 4CPA ion. This indicates that 4CPA moieties rearranges and assembles them selves for the formation of different monophasic nanohybrids, resulting in the formation of a well defined biphasic nanohybrid. The SEM and TEM images show a fiber like-structure. New part the chloride ion in the mixture media plays a role as competitor ion and because of its small size compared to the 4CPA ion it is easy to diffuse to the interior of the particles which make the intercalation by 4CPA more homogenous and highly crystalline intercalated ZnO. At the same time the ZnO peaks reduce in intensity compared to the more intense patterns of 4CPA intercalated with ZnO. Therefore it can be stated that the original layers of ZnO showed by XRD still kept their structure.

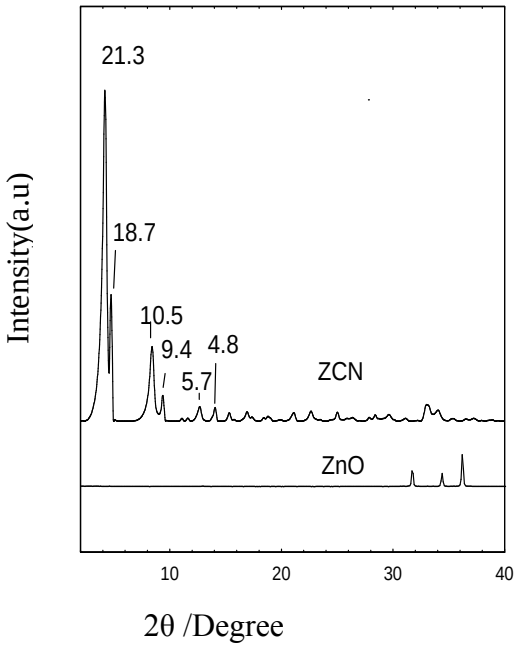

Fig[1] XRD pattern of ZnO and ZCN.

3.7 **FTIR Technique**

The presence of the herbicide anion 4CPA in to the nanohybrid can be verified by Fourier Transform Infrared Spectroscopy (FTIR). Fig. [2] presents the infrared spectra of 4CPA (top), ZnO (middle), ZCN (bottom) and. The broad absorption bands at 3455cm^{-1} arise from the stretching mode of OH groups in the ZnO layer and physisorbed water, ZCN nanocomposite this band appeared 3000 in the spectrum of 4CPA the shoulder at 3369 cm^{-1} confirmed the existence of hydrogen bonding between the water molecules and the ZnO layer. The band (1615cm^{-1}) attributed to stretching of the water molecule. The band at 2930cm^{-1} is attributed to C–H stretching vibration of intercalated 4CPA in ZCN, (from CH_2COO^- group), The peaks at 1546 and 1326 cm^{-1} are assigned to antisymmetric and symmetric stretching vibrations of the –COO- group on the pattern of both ZCN and 4CPA. The bands observed around 1487 and 1441 cm^{-1} correspond to the C=C bond of

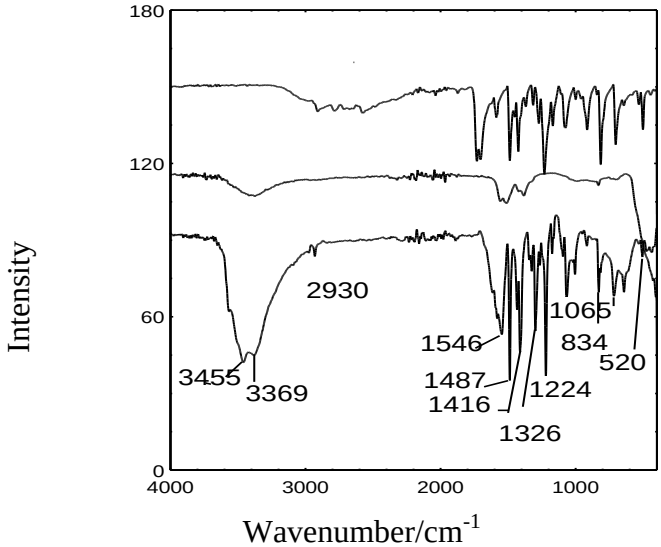

Fig [2] The FTIR spectrum of ZCN and ZnO in shows the characteristic peaks.

the aromatic ring of 4CPA in ZCN and 4CPA. The C-O-C anti symmetric and symmetric stretching bands appear at 1224 and 106 cm^{-1} in spectrum of 4CPA and ZCN.
The peaks and bands in the lower wave number region (i.e., 400–800 cm^{-1}) are due to M–O vibration and M–OH bending in the ZnO layers that can be clearly observed in both ZCN and ZnO FTIR spectra and the bands observed at 829cm^{-1} correspond to (CH_2) rocking. That is an indication of 4CPA intercalation in ZnO interlayer spaces and this is clearly observed with the appearance of the 2926 cm^{-1} band.

3.3 **SEM Morphology**:
As-prepared ZCN shows fiber-like structures various sizes and morphology. The morphology of ZCN samples obtained defer in morphology and shapes from that of commercial ZnO. Fig [3] shows SEM that synthesis of ZCN with initial concentration of 4CPA, A (0.4), B(0.05) for the resulted ZCN and (C) commercial ZnO, TEM images fig.[3.D] for ZCN these images shows, fiber-like morphology of ZCN samples synthesized by different concentrations. It is clear that with increasing concentrations of 4CPA more agglomeration takes place. As shown in the XRD well ordered pattern, with increasing concentrations of organic anion up to 0.4M resulted in well ordered white crystallized nanoparticles which is a general character for crystal growth SEM micrographs. ZCN showed micro-fiber morphology with uniform sized distribution of fiber structure and more aggregate was obtained at a concentration of 0.4M 4CPA. The SEM images of the ZCN.
In general, the initial 4CPA concentration probably controlled the shape of nanoparticles. The controlled and homogeneous growth of two phases may be due to the orientation of two growth phases. It may be that the initial molar ratio of 4CPA/ZnO in the solution is responsible for such phenomenon. However, the fibers were found to have some damaged surfaces as the concentration decreased to 0.05M. The effect of the initial 4CPA concentration on the morphology of ZCN is believed to be regulated by molar ratio. It was observed in TEM micrographs Fig [3D] of the as-prepared ZCN that the ZCN fiber had lengths ranging from 1300 to 1500 nm and about 250 nm in diameter.
The resulting intercalated ZCN nanofiber with high crystal quality is very important for application to research on nanocomposite devices.

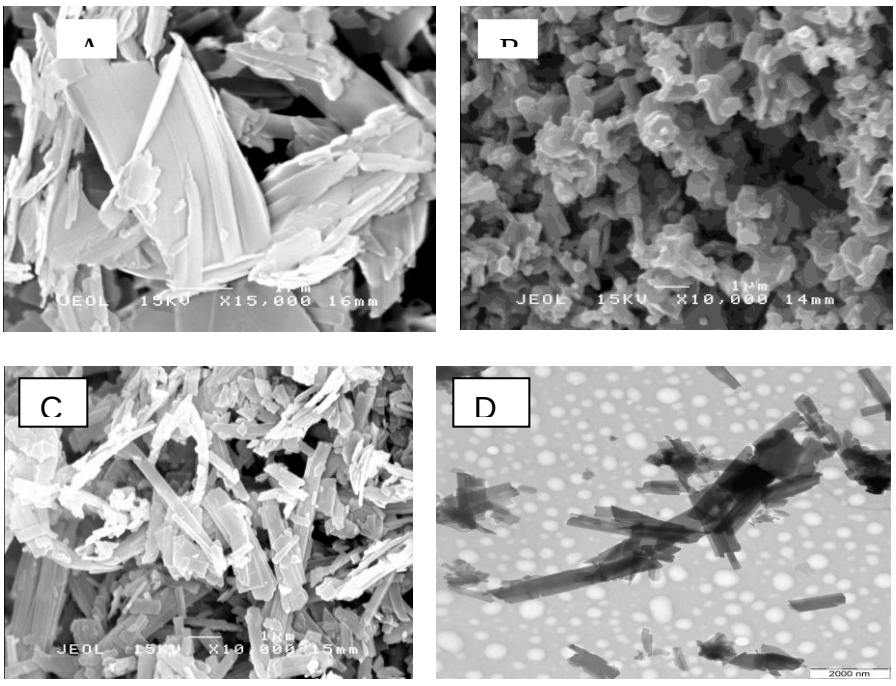

Fig [3] shows SEM for ZCN initial concentration of 4CPA, A(0.05M), B(ZnO) C (0.4M), TEM images (D) of ZCN.

3.4 **UV Energy Gap**

The UV-Visible spectrum of ZnO and the nanoparticles (ZCN), Fig. [4] shows high optical transmittance which is above 70% in the 400-800 nm wavelength range in the case of ZnO. The resulted ZCN has a new optical transmittance at wave length 226 nm E_{gap} = 4.86 eV, that can be obtained with the sample prepared by initial concentration of 4CPA at 0.05, 0.1, and 0.2M. The E_{gap} shifted to 4.71eV with increase in 4CPA ion concentration at 310 nm, E_{gap} = 4eV for the 0.05 and 0.1M concentrations

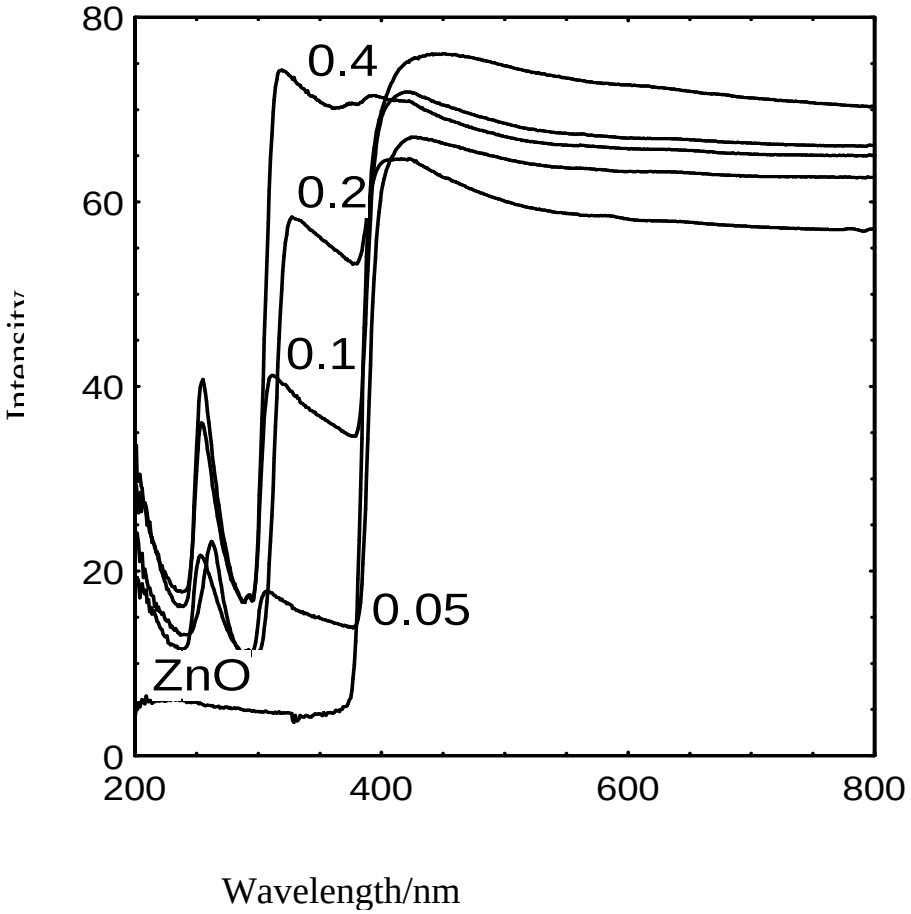

Fig [4] Shows UV-Vis. Energy gap from low to high, 0.05M, 0.1M, 0.2M and 0.4M of initial concentration of 4CPA to form ZCN.

These last absorptions were shifted to 319-328 nm with increasing ion concentration to 0.4M with E_{gap} = 3.78eV. The absorption edge of ZnO film also shifted to a shorter wavelength. This phenomenon indicates that the optical energy gap is enlarged with increase in ion concentration for the formation ZCN compared to ZnO and the blue shift adsorption edge is due to increase in concentration with optical energy gap .

3.5 **Thermal Analysis**

As shown in Fig [5] and table[1], shows the TG-DTG curves of ZCN, reveal three distinguishable weight loss steps, first step starts from 37 C^o terminating at 115 ^oC at a peak temperature of 84 ^oC. This is attributed to the loss of physically adsorbed and interlayer water. The second endothermic step is between 117-208 ^oC with its peak at 137 ^oC is attributed to the decarboxylation of 4CPA. The third endothermic step is between 221-520 ^oC with a maximum at 287 ^oC is attributed to decomposition of 4CPA. The last endothermic step between 590-910 ^oC with maximum at 822 ^oC is attributed to the removal of last traces of dehydroxylation of zinc layered hydroxide salts

accompanying the formation of ZCN. The CHNS analysis show that the ZCN was loaded 21.13% carbon and 8.26% hydrogen table [1]. Then the total loaded of 4CPA by ZCN is about 37.4%.ZnO %losses was 0.4% and pure 4CPA decompositions losses is in the range of % 99.7.

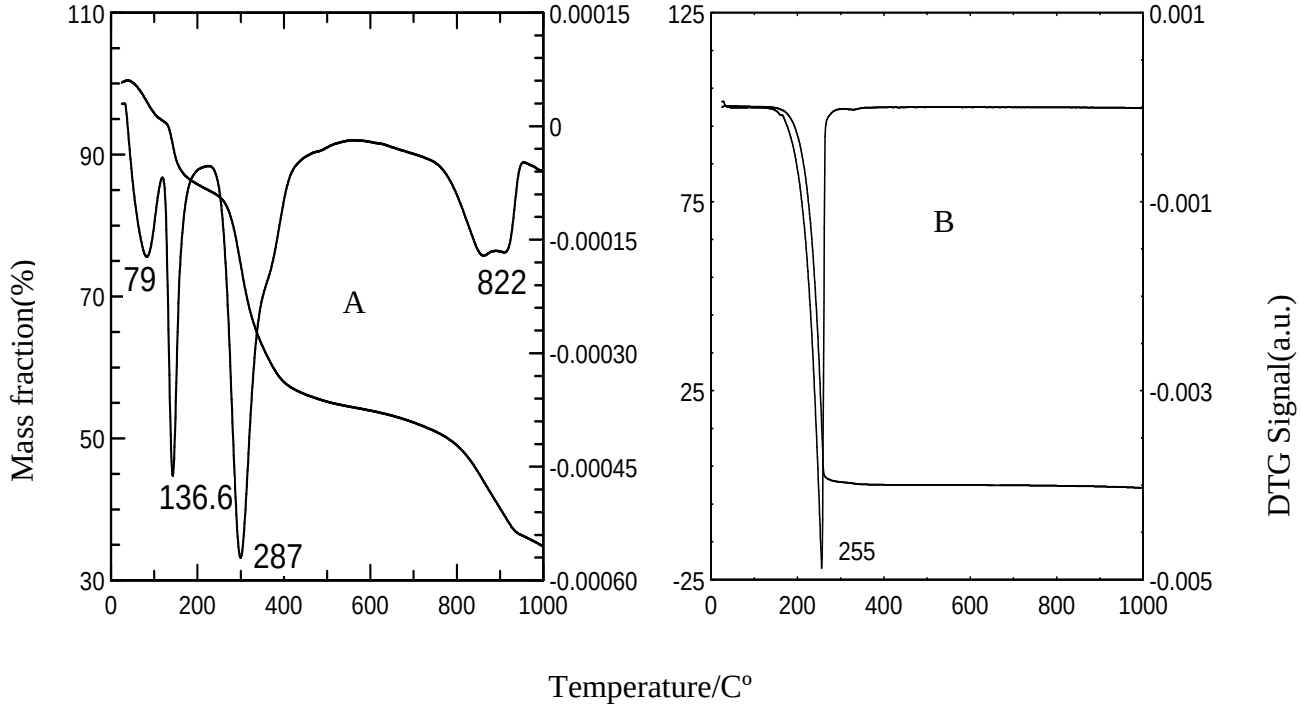

Fig[5] TG-DTG thermo grams curves shows the different phenomenon resulted from calcinations of ZCN (A), 4CPA (B), ZnO (C).

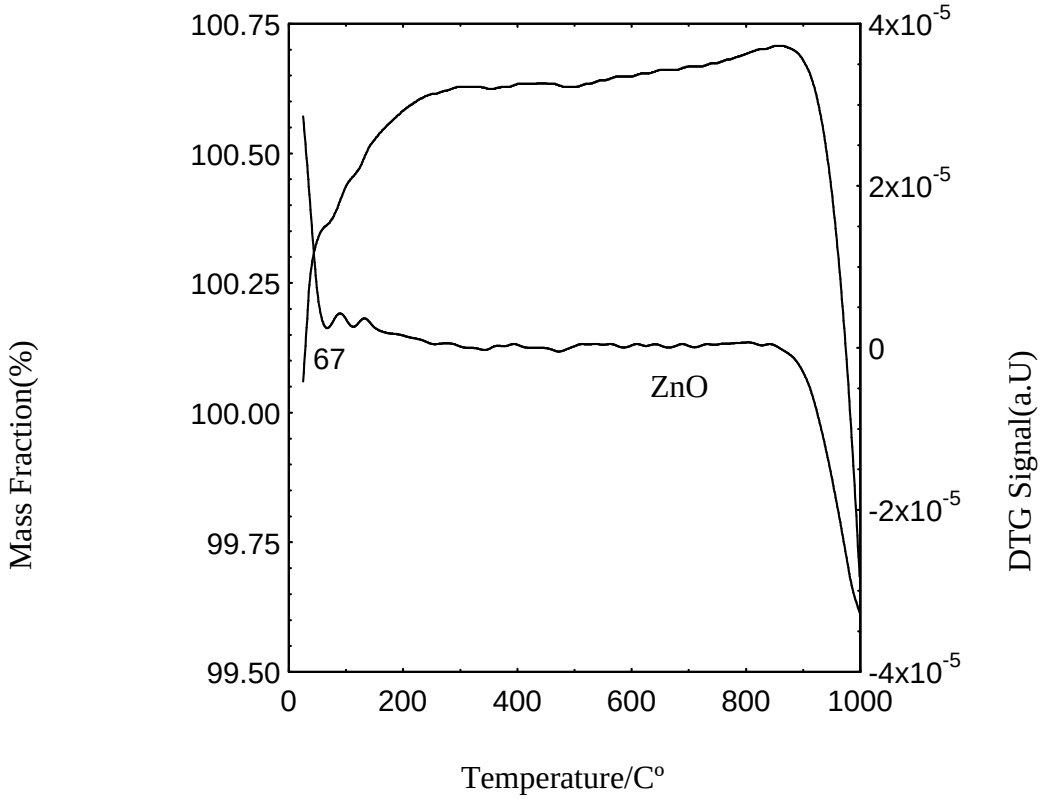

Table 1. shows the CHNS analysis, thermal analysis and UV-Vis. of solid absorptions

	Thermal Analysis			
^oC	First stage (C^o)	Second stage(^oC)	Third stage (^oC)	Fourth stage (^oC)
T_1-T_2	37-115	117-208	221-520	590-910
T_{max}	84	137	287	822
% Δm	8.69	37.58	4.38	10.35

ion initial	CHNS analysis		Uv.Vis. Absorption	
conc.	% C	% H	λ nm	E.gap
0.05 M	13.76	2.5	226	4.86
0.1 M	17.34	2.22	310	4
0.2 M	18.21	3.2	310	4
0.4 M	21.13	2.8	310	4

T_1=initial temperature, T_2 =final temperature, λ =wavelength in nm., initial con.=initial concentration of 4CPA, Δm=peak temperature.

3.8 Kinetic Study

The release of 4CPA from the interlayer of ZCN into aqueous solution at concentration 0.005M sodium carbonate . The accumulated 4CPArelease into the aqueous solution is 51%, 71%, 86% and 94% at time 260, 640, 1400 and 2000 minutes respectively, Fig. [6A]. 2000 min. of the release beginning is the equilibrium stage of release. Fitting the release data of 4CPA to first order Fig. [6B], pseudo second order Fig. [6C] and parabolic diffusion equations Fig[6D] shows that the pseudo second order model give the best fit with r^2 =1, and $t_{1/2}$ value of 990 min. compare to the first order model r^2=0.97 and $t_{1/2}$ =1386 min. The of parabolic diffusion model did not well fitted.

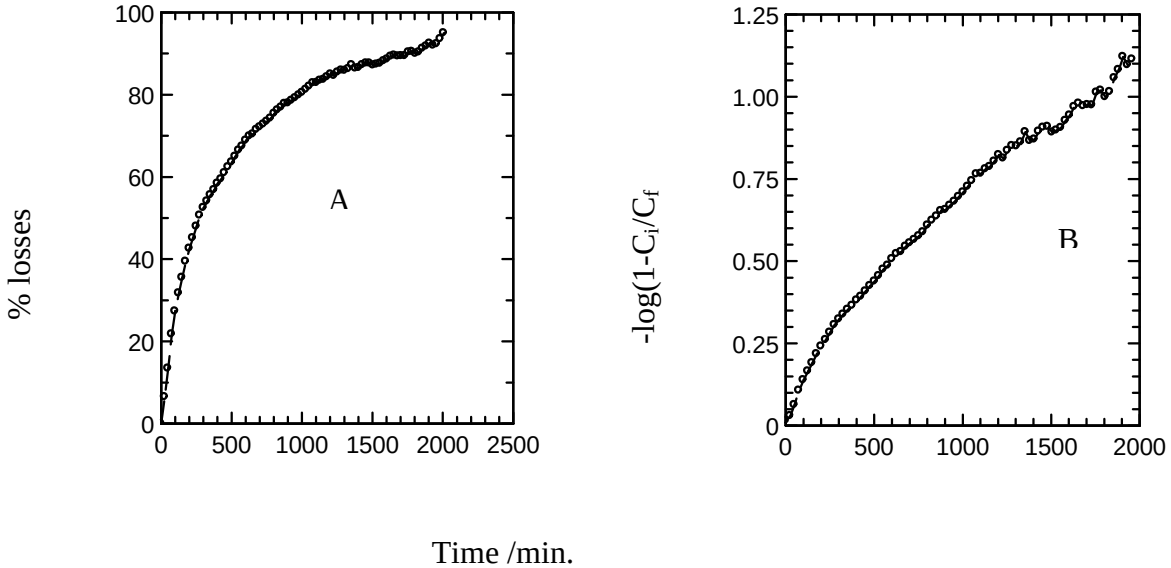

Fig [6] % Release (A), (C) pseudo second order (D) and parabolic diffusion model.

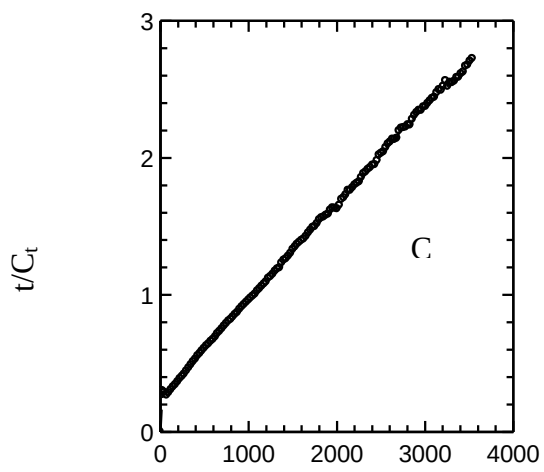

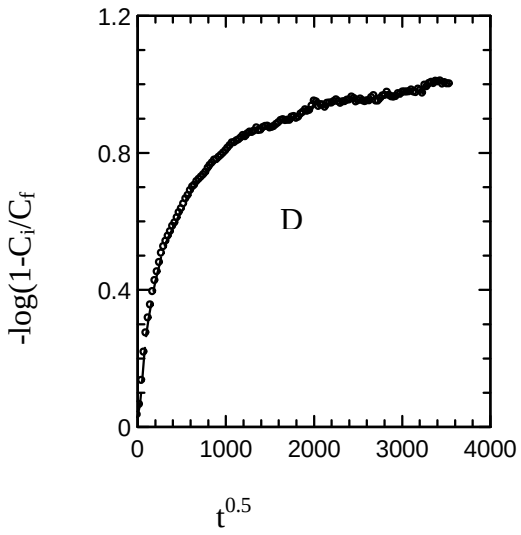

4.0 **Conclusion**

Direct synthesis of zinc-4-chlorophenoxy acetate-layered hydroxide nanohybrid by reaction of ZnO with 4-chlorophenoxy acetic acid in aqueous solution was found effective and simple for the formation of layered nanohybrid material. The controlled release study shows that the release process of the intercalated 4CPA from the nanohybrid is governed by pseudo second order, similar to other layered nanohybrides such as LDH-4CPA[13], LDH-Acid Fuchsin [14].

Acknowledgements

This work was funded by ITMA-UPM research grant fellowship(UPM/1.9.1), authors gratefully acknowledge ITMA-UPM.

5.0 **References**

[1] M. Z. Hussein, M. Y. Ghotbi, A. H. Yahaya, M. Z. Abd Rahman, Mater. Chem. Phys. 113 (2009) 491–496

[2] M. Z. Hussein, M. Y. Ghotbi, A. H. Yahaya, M. Z. Abd Rahman, Solid State Sci.11,2(2009)368-375.

[3] L. Zhang, Y. Ding, M. Povey, D. York, Progres. Nat. Sci. 18 (2008) 939–944.

[4] D. Guo, C. Wu, H. Jiang, Q. Li, X. Wang, B. Chen, J. Photochem. Photobio. B: Biolog. 93 (2008) 119–126.

[5] R. Wahab, S. G. Ansari, Y. S. Kim, M. A. Dar, H.S. Shin, J. All. Comp. 461 (2008) 66–71

[6] M. Y. Ghotbi, M. Z. Hussien, A. H. Yahya, M.Z. Abd Rahman, j . Phys. Chem. Solid. 70,(2009) 948-954.

[7] L.Y. Lin, H. J. Kim, D. E. Kim, Appl. Sur. Sci. 254 (2008) 7370–7376.

[8] Z. Wang, B. Huang, X. Qin, X. Zhang, P. Wang, J. Wei, J. Zhan, X. Jing, H. Liu, Z. Xu, H. Cheng, X. Wang, Z. Zheng,. Material. Lett. 63 (2009) 130-132.

.[9] R. Y. Hong, S. Z. Zhang, G. Q. Di, H. Z. Li, Y. Zheng, J. Ding, D. G. Wei, Res. Bull. 43 (2008) 2457–2468.

[10] Z. Huang, D. Yan, M. Yang, X. Liao, Y. Kang, G. Yin, Y. Yao, B. Hao, J. Colloi. Inter. Sci. 325 (2008) 356–362.

[11] M. Wang, Y. Lian, X. Wang,. Curr. Appl. Phys. 9 (2009) 189–194.

[12] R. Ullah, J. Dutta, J. Hazar. Mater. 156 (2008) 194–200. 3420.

[13] M. Z. Hussein, A. Yahaya, Z. Zainal and L. H. Kian, Sci. Technol. Adv. Mater. 6(2005)956-962.

[14] M. Z. Hussein, A. Yahya, M. Shamsul, H. M Salleh, T. Yap, J. Kiu, J. Mater. Letter.58, (2004) 329-332.